

Implementation into OpenSees of XFEM for Analysis of Crack Propagation in Brittle Materials

*Original*

Implementation into OpenSees of XFEM for Analysis of Crack Propagation in Brittle Materials / Fichera, S., Biondi, B., Ventura, G.. - ELETTRONICO. - 326:(2023), pp. 157-165. (EOS 2022: 2022 Eurasian OpenSees Days Torino (Italia) 07/07/2022 - 08/07/2022) [10.1007/978-3-031-30125-4\_14].

*Availability:*

This version is available at: 11583/2979255 since: 2023-06-19T17:15:11Z

*Publisher:*

Springer

*Published*

DOI:10.1007/978-3-031-30125-4\_14

*Terms of use:*

This article is made available under terms and conditions as specified in the corresponding bibliographic description in the repository

*Publisher copyright*

(Article begins on next page)

# Computational flow models for crystallization processes

Daniele Marchisio<sup>1</sup>, Andrea Querio<sup>1</sup> and Antonello Raponi<sup>1,2</sup>

Crystallization is a key separation and purification method governed by thermodynamics, kinetics, and multiphase fluid dynamics. Supersaturation generation, nucleation, crystal growth, aggregation, and breakage determine particle size and shape and are described using population balance models (PBMs). Coupled with computational fluid dynamics (CFD), PBMs enable spatially resolved predictions of particulate behavior in real reactors. This review outlines fundamental crystallization kinetics and PBM formulations, including nucleation and growth expressions, aggregation and breakage kernels, and moment-based solution methods. It also highlights how multiphase CFD represents turbulence, mixing, and phase interactions in stirred tanks, tubular reactors, static mixers, and impinging jets, supporting process design and scale-up. Key computational challenges include stiffness, micro-mixing, reaction–equilibrium networks, and parallelization, along with cost-reduction strategies such as compartment models and CFD-informed reactor representations. Emerging machine-learning tools accelerate parameter estimation and surrogate modeling, with applications from inorganic precipitation to pharmaceutical crystallization.

## Addresses

<sup>1</sup> Department of Applied Science and Technology, Politecnico di Torino, Torino, Italy

<sup>2</sup> Centre SPIN, CNRS UMR 5307 Laboratoire Georges Friedel, Mines Saint-Etienne, France

Corresponding author: Marchisio, Daniele ([daniele.marchisio@polito.it](mailto:daniele.marchisio@polito.it))

Current Opinion in Chemical Engineering 2026, 52:101246

This review comes from a themed issue on **Computational flow models to real-world reactors**

Edited by **Vivek Ranade** and **Ashwin Patwardhan**

Available online xxxx

<https://doi.org/10.1016/j.coche.2026.101246>

2211–3398/© 2026 The Authors. Published by Elsevier Ltd. This is an open access article under the CC BY license (<http://creativecommons.org/licenses/by/4.0/>).

## Introduction

Crystallization is a key separation and particle-formation process in which supersaturation, generated by chemical reaction, solvent exchange, cooling, or their combination,

leads to the formation of a new solid phase. The resulting solid may be crystalline or amorphous and may consist of a single compound or multiple components, as in co-crystals. In industrial practice, crystallization is widely employed as a unit operation for purification and product design, while in other contexts it is undesirable, as in scaling and fouling phenomena occurring in heat exchangers and membrane systems. The fundamental thermodynamics, kinetics, and population balance theory underlying crystallization have been extensively covered in classical textbooks and reviews [1–3]. However, the translation of this knowledge into predictive tools for real-world turbulent reactors remains a major challenge. In particular, the strong coupling between hydrodynamics, supersaturation fields, and particulate processes requires computational frameworks that integrate multiphase computational fluid dynamics (CFD) with population balance modeling (PBM).

This review focuses specifically on this coupling. Rather than reiterating established crystallization theory, we examine: (i) the hierarchical relationship between generalized population balance equations, PBM, and two-fluid CFD models; (ii) practical strategies for CFD–PBM coupling in turbulent systems; (iii) computational bottlenecks and cost-reduction techniques, including operator splitting and parallelization; (iv) reduced-order and CFD-informed models for scale-up and (v) emerging directions such as machine-learning-assisted parameter identification and surrogate modeling.

## Thermodynamics and kinetics of crystallization

Once the solubility limit is overcome, the solution is supersaturated. Supersaturation,  $S = c/c_s$ , is locally defined as the ratio between the actual concentration of a chemical species,  $c$ , and its solubility,  $c_s$ . Solubility depends on temperature and on the crystalline form (e.g. polymorph, hydrate, amorphous phase). In multi-component systems, it is typically represented through phase diagrams, which guide crystallization process design. Supersaturation is the driving force for crystallization and, when greater than unity, enables nucleation. Nucleation may be classified as primary (in the absence of crystals of the same compound) or secondary (in their presence). Primary nucleation can further be homogeneous or heterogeneous, and its rate is commonly described using classical nucleation theory.

$$J(S) = A \exp\left(-\frac{B}{(\ln S)^2}\right) \quad (1)$$

where  $A$  and  $B$  depend on temperature and can be derived from theory or inferred from experiments, using well-defined protocols which rely on the stochastic nature of nucleation [4]. Once the nuclei are formed, they can grow because of molecular growth, whose rate depends on the controlling mechanisms and is usually described with the following empirical equation:

$$G(S) = k_g (S - 1)^g \quad (2)$$

where again the parameters  $k_g$  and  $g$  can be derived from single crystal experiments or inferred from larger-scale crystallization experiments.

Grown particles can then undergo aggregation and breakage. In turbulent systems, particle collisions and shear-induced breakage are strongly influenced by the turbulent dissipation rate,  $\varepsilon$ , which quantifies the intensity of turbulent fluctuations. Aggregation and breakage kernels often incorporate turbulence effects, providing practical estimates of collision frequency, adhesion efficiency, and fragment distribution under realistic turbulent flow conditions. In this case, the aggregation rate is defined via its kernel, which for particles larger than the Kolmogorov length-scale, is defined as follows:

$$\beta(L, \lambda) = \left( \frac{2k_B T}{3\mu} \frac{(L + \lambda)^2}{L\lambda} + C_T \cdot 2.2943 \sqrt{\frac{\varepsilon}{\nu}} (L + \lambda)^3 \right) \quad (3)$$

where  $k_B$  is the Boltzmann constant,  $T$  is the temperature,  $\mu$  is the dynamic viscosity of the suspending liquid,  $\nu$  is its kinematic viscosity, and  $L$  and  $\lambda$  are the characteristic sizes of the colliding and aggregating particles. The parameter  $C_T$  accounts for non-idealities and must be determined by fitting with experiments. This kernel describes the collision frequency arising from Brownian motion and turbulent fluctuations. It is typically multiplied by an aggregation efficiency accounting for the probability of successful adhesion upon collision. Further details can be found in the literature [5]. Other relevant particulate processes include breakage and secondary nucleation. In breakage, particles fragment into smaller pieces; its kinetics is described by a breakage kernel, defining the breakage rate, and a fragment distribution function, specifying the number and size of the resulting fragments [6]. The term secondary nucleation may refer either to attrition, namely the detachment of small fragments from existing particles, or to nucleation from solution promoted by the surface of crystals of the same compound. The latter mechanism remains not fully understood, although recent first principles and experimental studies have proposed rate expressions [7–10].

### Population balance modeling

The kinetics of nucleation, growth, aggregation, and breakage determine the final particle characteristics:

size, shape, and form. Notably, the particle size distribution (PSD) and the particle size and shape distribution are described via a governing equation, called the population balance equations (PBE), which can be solved with different numerical methods, resulting in a PBM [11–13]. A comprehensive description of the theory behind this equation can be found in the literature [6,14]. This is a partial integro-differential equation that operates on a distribution function, formulated via an ensemble averaging procedure, that in turn defines how the particles are distributed over some internal coordinates, notably size. Mono-variate (one-dimensional) PBEs employ only one internal coordinate; multivariate (multidimensional) PBEs employ more than one internal coordinate. Since the computational costs of standard discretization techniques (i.e. finite difference, finite volume, finite elements) escalate as the number of internal coordinates increases, one interesting solution method, especially for computational flow models, is the method of moments. With this method, the PSD is described in terms of some moments, which in the monovariate case are defined as follows:

$$m_k(t, \mathbf{x}) = \int_0^\infty n(L, t, \mathbf{x}) L^k dL \quad (4)$$

reducing the dimensionality of the problem by integrating the internal coordinate particle size,  $L$ . The governing equations are hierarchically related: the generalized population balance equation (GPBE) defines the evolution of the full particle distribution, including velocity. Integrating over velocity yields the classical PBE, and applying moment transforms produces the moment-based form used in two-fluid CFD models. Moments represent physical measurable quantities, such as total particle number density (i.e.  $m_0$ ), particle specific surface area ( $m_2$ ), and particle volume fraction ( $\alpha_p$ , related to  $m_3$ ), whereas the ratio of two moments defines a mean particle size. For example,  $d_{10} = m_1/m_0$  is the number-averaged particle size,  $d_{21}$  the length-averaged particle size,  $d_{32}$  the area-averaged particle size (or Sauter diameter), and  $d_{43}$  the volume-averaged particle size. The use of these four mean particle sizes is equivalent to considering, for numerous applications, the entire PSD. The evolution of the moments of the PSD is governed by a standard transport equation:

$$\frac{\partial m_k}{\partial t} + \mathbf{u}_p \cdot \nabla m_k = \nabla \cdot (D_t \nabla m_k) + \bar{S}_k \quad (5)$$

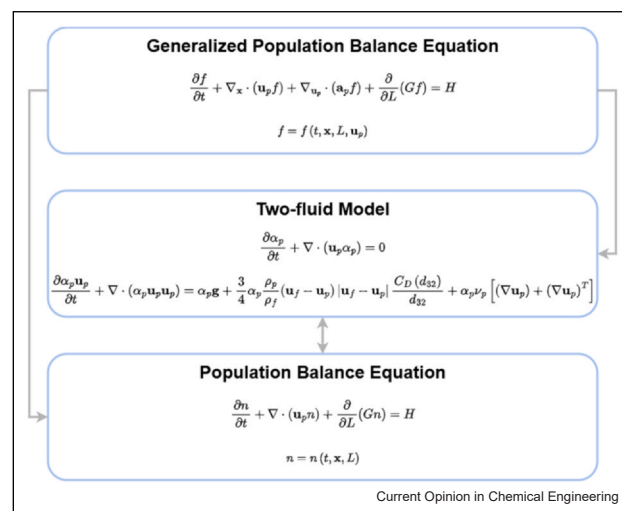
With the usual terms accounting for accumulation, convection, and diffusion.  $\mathbf{u}_p$  and  $D_t$  are respectively the particle velocity and (turbulent) diffusivity, whereas  $\bar{S}_k$  is the source term accounting for nucleation, growth, aggregation, and breakage. A closure problem arises both in the transport and source terms when size dependencies are present. This can be overcome by using a quadrature approximation [6,15]. The equation can be

solved by using the finite-volume approach in combination with strategies to speed up the simulation, such as operator-splitting, and to preserve the moment realizability, as described in the literature [14,16]. While tracking moments reduces computational cost, it introduces a trade-off: fine details of the PSD may be lost, limiting accuracy for certain applications. However, ratios of moments can define key particle sizes (e.g. number-average  $d_{10}$ , Sauter diameter  $d_{32}$ ) sufficient for most engineering purposes.

### Multiphase flow effects, computational fluid dynamics, and coupling with the population balance model

Crystallization processes are multiphase systems in which fluid dynamics plays a big role. Independently from how supersaturation is generated (e.g. solvent-displacement, cooling crystallization, reactive crystallization) very often supersaturation is not spatially homogeneous and uniform across the crystallizer, which can be batch, continuous or semi-batch, and have the form of a stirred tank [17,18], a tubular reactor [19,20], with or without inserts, as in the case of static mixers [21], or a confined impinging jet crystallizer [22,23]. This latter category has become very popular in crystallization lately, especially to produce lipidic nanoparticles for the delivery of mRNA vaccines [24]. Geometrical details of the crystallizer and operating conditions (i.e. stirring rate, impinging jet velocity, cooling rate, etc.) can affect the flow field, the spatial distribution of supersaturation, and therefore the final particle characteristics. This is particularly evident during scale-up (and down) and during the transfer of a process from one piece of equipment to another. The same ‘chemical recipe’ can result in very different particle characteristics when the scale or the geometry of an impeller is even only slightly modified. Fluid dynamics heavily affects the final particle characteristics also because it determines the rate with which particles collide (and therefore aggregate) and the type and rate of deformation of the fluid (or shear rate), which in turn defines the rate of breakage of the crystals. In turbulent systems, these phenomena are compactly and efficiently described by the turbulent dissipation rate,  $\epsilon$ , which is the rate with which turbulence is generated and dissipated by viscosity. This can also be thought as the power input per unit mass in the crystallizer and is usually estimated by using multiphase turbulent models, such as the two-equation  $k - \epsilon$  models in the context of Reynolds-averaged Navier-Stokes equations (RANS) or in the context of large eddy simulations (LES) approaches. RANS provides time-averaged fields with lower computational cost, while LES resolves large eddies and offers higher fidelity at the expense of increased runtime and equation counts, often reaching millions of coupled PDEs per time step for industrial-scale systems [25].

Figure 1



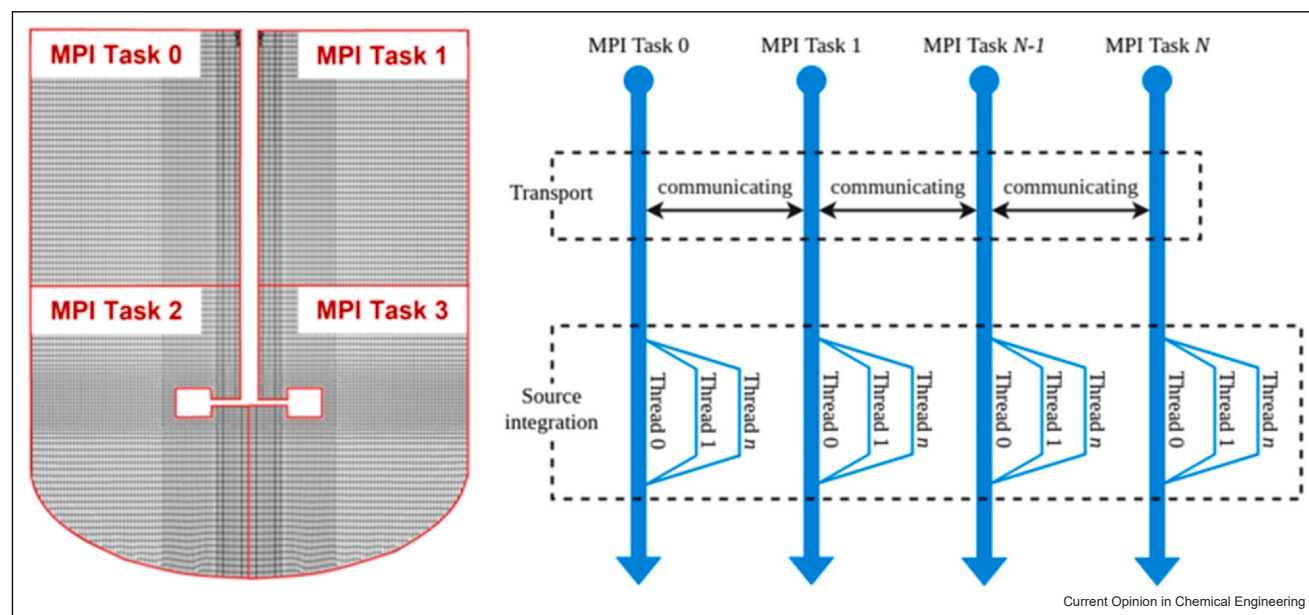
Hierarchical relationship between governing equations. The PBE is derived by integrating out particle velocity,  $u_p$ , from the GPBE. The governing equations of the two-fluid model, namely the continuity equation (top) and the moment balance equation (bottom) for the disperse particulate phase, are also derived from the GPBE by applying moment transforms of different order. This hierarchical relationship between these governing equations defines the way in which these equations should be coupled [6].

The multiphase nature of crystallization systems has been neglected for many years, and only three decades ago, the crystallization community started fully acknowledging the importance of multiphase fluid dynamics. The complex interplay between particulate processes and fluid flow requires the use of computational flow models based on multiphase CFD. Among the different CFD models and approaches available [26,27], Eulerian-Eulerian CFD models are the most suited for simulating real-world industrial-scale crystallization reactors. The two-fluid (and the multi-fluid) model is based on the solution of mass and momentum balance equations for the phases involved, the continuous liquid phase and the solid particulate phase. The theoretical framework under which these models operate (see Figure 1), their correct and well-posed formulation, and the proper way in which they should be interfaced with PBM have been only recently fully clarified [28–30].

### Computational challenges and anchoring to real-world reactors

One of the main issues that hinders the uptake of computational flow models in crystallization for addressing real-world reactors is the associated computational cost. With the increase of computational power, thanks to high-performance computing (HPC) facilities, this problem has partially been solved; very efficient parallelization strategies must be developed, as increasing the

Figure 2



A possible hybrid parallelization scheme [16]. Message Passing Interface (MPI), a standard for parallel computing, is used to divide the computational domain into regions (domain decomposition) and assign them to different tasks and processors. Thanks to the operator-splitting procedure this takes care of the transport terms of the governing equations, see for example Eq. (5). OpenMP, which supports multi-platform shared-memory parallel programming, is used to parallelize the time-integration of the source term into different threads.

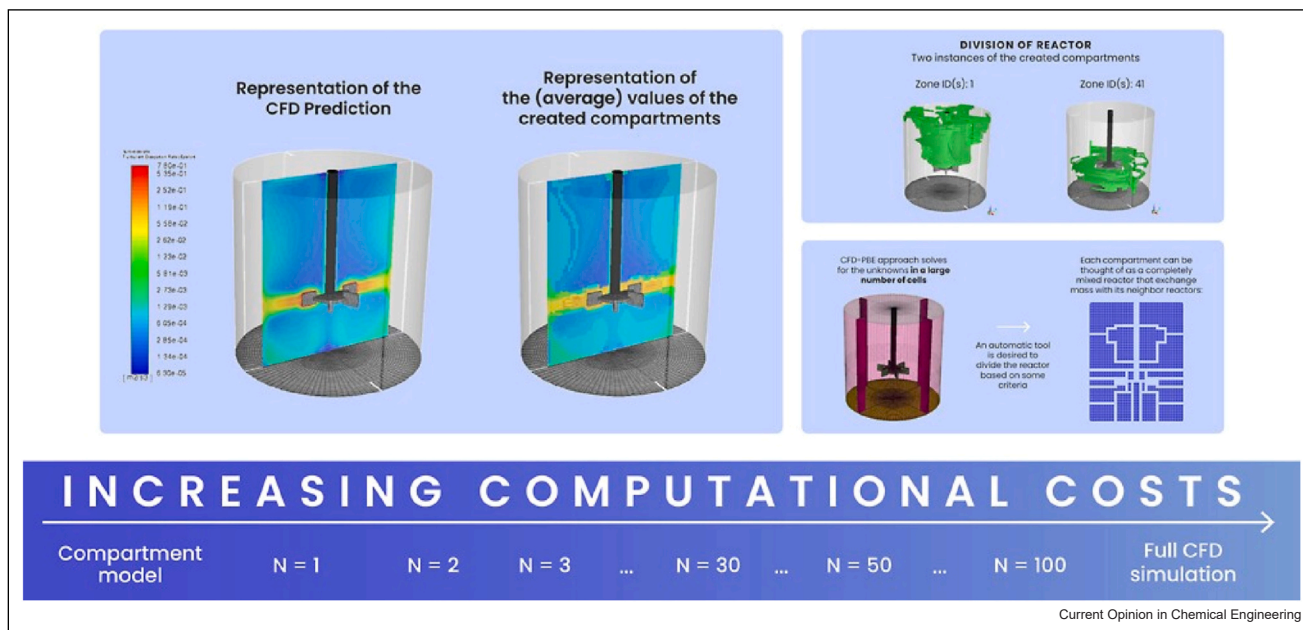
number of parallel processes sometimes causes large processor load imbalances, nullifying the beneficial effects of parallelization.

Even with efficient and extensive parallelization (see e.g. Figure 2), in some cases simplified flow models must be employed. This is particularly true when numerous phenomena must be accounted for. In many crystallization applications, for example, fast chemical reactions or nucleation processes are involved, requiring the use of so-called micro-mixing models. These reconcile the existence of turbulent fluctuations in supersaturation with turbulence models based on Reynolds or spatial averaging procedures, as in the case of RANS and LES models. Additionally, very often, to properly evaluate supersaturation, many chemical species in solutions must be accounted for, often linked with each other via complex chemical equilibria. In conjunction with, again, an operator splitting procedure, one must couple the CFD simulation, solving the chemical species transport equations, with the simultaneous resolution of these many chemical equilibria, with, for example, a Newton-Rapson procedure, slowing down the simulation and increasing the computational costs [5]. Finally, especially when very high supersaturations are reached, supersaturation must be evaluated using activity coefficients, with an additional burden to the computational costs. In these scenarios (see Figure 3), it is interesting to explore simplified computational flow

models, such as CFD-informed mixed-suspension mixed product removal (MSMPR) models, or CFD-informed plug flow reactor models [5,31,32]. An interesting alternative is the use of compartment models, where one single CFD simulation is used to generate a limited number of compartments, sharing similar values of supersaturation and/or turbulent dissipation rate, respectively driving forces for nucleation & growth, and aggregation & breakage [16]. Some theoretical issues still need to be reconciled, as the governing equations of the CFD model and of the compartment model are different, as compartments exchange fluid elements and particles via convection only, whereas in the CFD simulation, the effect of (turbulent) diffusion is also considered. Other techniques do not suffer from these shortcomings [33,34].

Machine learning and artificial intelligence [36–38] offer a great opportunity here as they can greatly accelerate one of the bottlenecks of model development, namely the identification of the PBM parameters of the CFD-PBM simulation. High-fidelity CFD-PBM simulations can require hours to days of computation for industrial-scale systems [39]. Estimating these parameters through direct optimization over high-fidelity CFD-PBM simulations can be computationally prohibitive. A practical alternative consists of constructing a surrogate model trained on CFD-PBM data and employing it in inverse mode to perform multivariate optimization more

Figure 3



Simplified fluid dynamic models. From left to right: detailed CFD simulations are run on the computational domain. These are then used to divide the domain into a limited number of compartments using, for example, the agglomerative clustering algorithm of Scikit-learn [35]. The compartment model targets a specific property, for example supersaturation, or the turbulent dissipation rate. The number of compartments can be varied from one, namely the entire vessel is described as one perfectly well-mixed system, to 10, 20 up to, the total number of cells of the original CFD simulation, resulting again in the original CFD simulation.

efficiently. In such frameworks, the neural network is trained to map characteristic outputs (e.g. particle sizes) to kinetic parameters, enabling rapid parameter identification. This strategy reduces the computational cost of calibration by orders of magnitude compared to direct optimization and has been successfully demonstrated in the context of multivariate optimization of precipitation kinetics using deep-learning-assisted inverse design of CFD-PBM simulations [40]. Training such surrogates requires an upfront investment in generating CFD-PBM datasets, and their applicability is generally system-specific: transfer to new reactor geometries or operating conditions may necessitate retraining. Nevertheless, these approaches enable rapid parameter identification and design space exploration while retaining physical consistency, bridging the gap between detailed simulations and practical process optimization [41].

### Real-world reactors and applications

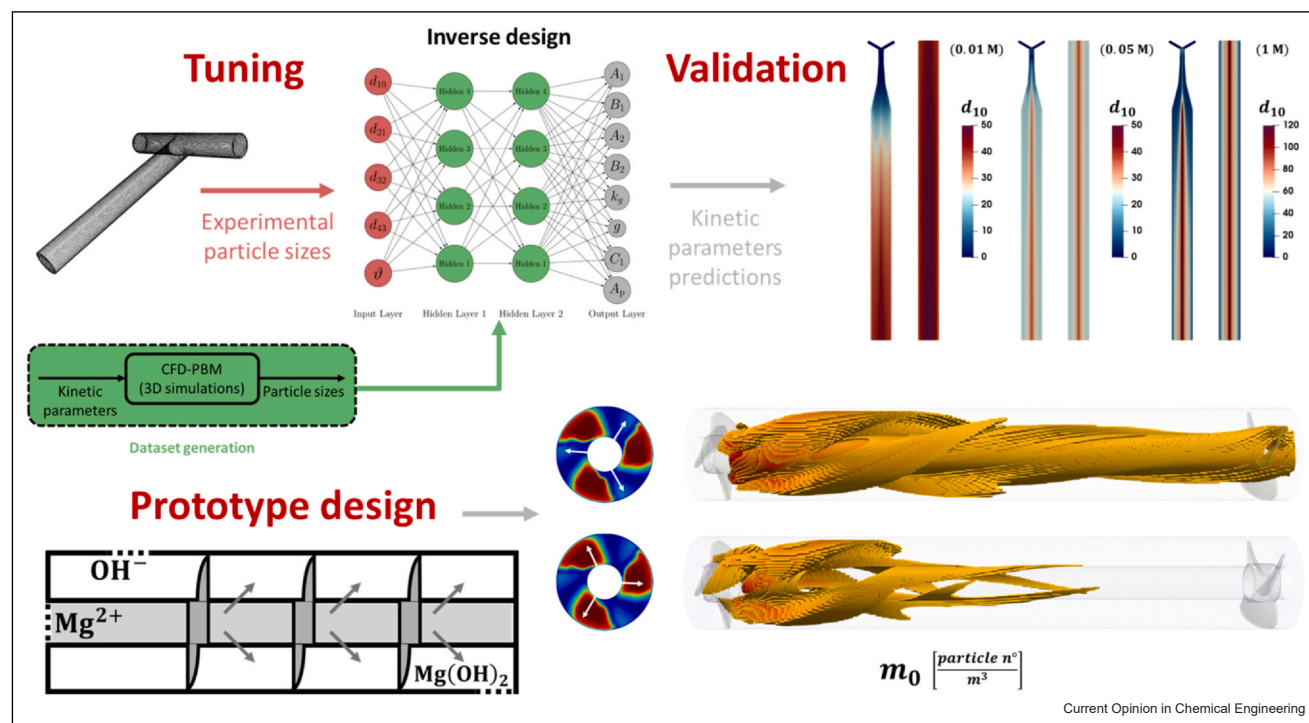
The models previously described have been extensively used to design, optimize, and scale up crystallization reactors. They are particularly useful for reactive crystallization, or precipitation processes, where the time-scales associated with the particulate processes are very close to those of the fluid flow, resulting in a complex interplay between particle formation and evolution, and multiphase fluid dynamics.

For example, a prototype for the extraction, via crystallization, of magnesium hydroxide has been developed by using a validated CFD-PBM model [42] (see Figure 4). CFD-PBM has also been extensively employed to study the production process of nickel, manganese, and cobalt hydroxides, very popular precursors for cathode active material (pCAM). The effect of impeller type and shape on the PSD, density, and form of the pCAM particles has been investigated deeply [5,43–45].

These computational flow models are also very useful in the case of solvent-displacement, where a solution of a solute in a solvent is mixed with an anti-solvent, resulting in very high supersaturation and super-fast particle formation. In solvent displacement, it is particularly challenging to understand the separate effects of solvent choice on solubility and on mixing dynamics. CFD and PBM models are particularly useful in this area to guide the solvent selection [48,49], especially for pharmaceutical applications [21,24,50] where reactant costs are extremely high.

CFD coupled with PBM and within multiscale and hybrid models is also very useful in the case of slug flow crystallization [51,52] or in assessing the validity of perfect mixing assumptions often made in laboratory equipment used to measure solubility and nucleation kinetics [53].

Figure 4



Validation of a typical PBM coupled with CFD. The figure shows two contributions found in the literature. The upper part of the figure shows a multivariate optimization performed with deep learning that allows the calibration of a 3D CFD-PBM model [46]. The lower part, on the other hand, uses the validated 3D CFD-PBM model for the design and performance optimization of an innovative prototype for magnesium hydroxide precipitation [47].

CFD can further be employed, for example, to identify the optimal withdrawal position in large stirred tank crystallizers [54] or to predict clogging and fouling [55] hindering the productivity of numerous industrial crystallization processes.

## Conclusions

Computational flow models have matured into practical tools for simulating real-world crystallization reactors. Their most efficient implementation combines CFD with PBM, leveraging strategies such as operator-splitting and parallelization to reduce computational costs. In cases where even HPC cannot achieve acceptable run-times, typically on the order of hours rather than days for industrial-scale simulations, simplified CFD-informed models, such as compartment or MSMR-based approaches, provide practical alternatives. Machine learning and artificial intelligence are expected to play an increasingly important role, both by serving as surrogates for detailed simulations and by incorporating physical constraints, enabling faster parameter identification and exploration of operational space while taking advantage of modern GPU-accelerated HPC architectures.

## Data Availability

Data will be made available on request.

## Declaration of Competing Interest

The authors declare that they have no known competing financial interests or personal relationships that could have appeared to influence the work reported in this paper.

## References and recommended reading

Papers of particular interest, published within the period of review, have been highlighted as:

- of special interest
- of outstanding interest

1. Mullin JW: *Crystallization*. edn 4, Butterworth-Heinemann; 2001.
2. In *Handbook of Industrial Crystallization [Internet]*. Edited by Myerson AS, Erdemir D, Lee AY. edn 3, Cambridge University Press; 2019, <https://doi.org/10.1017/9781139026949>
3. Rudolph P: **Crystal growth fundamentals: kinetics of crystallization**. De Gruyter; 2025, <https://doi.org/10.1515/9783111714226>
4. Jiang S, Ter Horst JH: **Crystal nucleation rates from probability distributions of induction times**. *Cryst Growth Des* 2011, 11:256-261, <https://doi.org/10.1021/cg101213q>

5. Shiea M, Querio A, Buffo A, Boccardo G, Marchisio D: **CFD-PBE modelling of continuous Ni-Mn-Co hydroxide co-precipitation for Li-ion batteries.** *Chem Eng Res Des* 2022, **177**:461-472, <https://doi.org/10.1016/j.cherd.2021.11.008>
6. Marchisio DL, Fox RO: *Computational Models for Polydisperse Particulate and Multiphase Systems*. edn 1, Cambridge University Press; 2013, <https://doi.org/10.1017/CBO9781139016599>
7. Cashmore A, Georgoulas K, Boyle C, Lee M, Haw MD, Sefcik J: **Secondary nucleation of  $\alpha$ -glycine induced by fluid shear investigated using a couette flow cell.** *Cryst Growth Des* 2024, **24**:4975-4984, <https://doi.org/10.1021/acs.cgd.4c00130>.  
This study uses a Couette flow cell to investigate how fluid shear triggers secondary nucleation of  $\alpha$ -glycine. Results clarify the relationship between shear conditions and nucleation rates, improving understanding of mechanically induced crystallization.
8. Bosetti L, Ahn B, Mazzotti M: **Secondary nucleation by interparticle energies. I. Thermodynamics.** *Cryst Growth Des* 2022, **22**:87-97, <https://doi.org/10.1021/acs.cgd.1c00927>
9. Ahn B, Bosetti L, Mazzotti M: **Secondary nucleation by interparticle energies. II. Kinetics.** *Cryst Growth Des* 2022, **22**:74-86, <https://doi.org/10.1021/acs.cgd.1c00928>
10. Ahn B, Bosetti L, Mazzotti M: **Secondary nucleation by interparticle energies. III. Nucleation rate model.** *Cryst Growth Des* 2022, **22**:3625-3636, <https://doi.org/10.1021/acs.cgd.1c01314>
11. Omar HM, Rohani S: **Crystal population balance formulation and solution methods: a review.** *Cryst Growth Des* 2017, **17**:4028-4041, <https://doi.org/10.1021/acs.cgd.7b00645>
12. In *The Handbook of Continuous Crystallization [Internet]*. Edited by Yazdanpanah N, Nagy ZK. The Royal Society of Chemistry; 2020, , <https://doi.org/10.1039/9781788013581>
13. Randolph AD, Larson MA: *Theory of Particulate Processes [Internet]*. Elsevier; 1971, <https://doi.org/10.1016/B978-0-12-579650-7.X5001-5>
14. Shiea M, Buffo A, Vanni M, Marchisio D: **Numerical methods for the solution of population balance equations coupled with computational fluid dynamics.** *Annu Rev Chem Biomol Eng* 2020, **11**:339-366, <https://doi.org/10.1146/annurev-chembioeng-092319-075814>
15. Fox RO, Laurent F, Passalacqua A: **The generalized quadrature method of moments.** *J Aerosol Sci* 2023, **167**:106096, <https://doi.org/10.1016/j.jaerosci.2022.106096>
16. Querio A, Shiea M, Buffo A, Marchisio DL: **Comparison between compartment and computational fluid dynamics models for simulating reactive crystallization processes.** *Ind Eng Chem Res* 2024, **63**:21991-22004, <https://doi.org/10.1021/acs.iecr.4c01483>.  
In this publication the difference between a CFD crystallization model and a compartment crystallization model is investigated. The key differences in the governing equations are explained, and strategies to reconcile the results between the two approaches are discussed.
17. Romano S, Trespi S, Achermann R, Battaglia G, Raponi A, Marchisio D, et al.: **The role of operating conditions in the precipitation of magnesium hydroxide hexagonal platelets using NaOH solutions.** *Cryst Growth Des* 2023, **23**:6491-6505, <https://doi.org/10.1021/acs.cgd.3c00462>
18. Ramezani K, Fonte CP, Rajagopalan AK: **Toward predictive modeling of industrial crystallizers: a compartmental framework for coupling hydrodynamics and population dynamics.** *Chem Eng Res Des* 2025, **224**:452-466, <https://doi.org/10.1016/j.cherd.2025.11.020>
19. Raponi A, Fida D, Vicari F, Cipollina A, Marchisio D: **Computational fluid dynamics and population balance model enhances the smart manufacturing and performance optimization of an innovative precipitation reactor.** *Processes* 2025, **13**:1721, <https://doi.org/10.3390/pr13061721>
20. Sulttan S, Rohani S: **Coupling of CFD and population balance modelling for a continuously seeded helical tubular crystallizer.** *J Cryst Growth* 2019, **505**:19-25, <https://doi.org/10.1016/j.jcrysgro.2018.10.012>
21. Aprile G, Pandit AV, Albertazzi J, Eren A, Capellades G, Thorat AA, et al.: **Loop-configuration for plug flow crystallization process development.** *Cryst Growth Des* 2023, **23**:8052-8064, <https://doi.org/10.1021/acs.cgd.3c00819>.  
The work introduces a looped tubular crystallizer with static mixers that mimics long residence times. Inline PAT monitoring and CFD simulations confirm plug-flow behavior with negligible backmixing, enabling efficient screening of nucleation through equilibrium in a compact setup. Demonstrated across multiple antisolvent crystallizations, the method cuts raw material requirements by 50–98% and can also support semi-continuous manufacturing.
22. Devos C, Mukherjee S, Inguva P, Singh S, Wei Y, Mondal S, et al.: **Impinging jet mixers: a review of their mixing characteristics, performance considerations, and applications.** *AIChE J* 2025, **71**:e18595, <https://doi.org/10.1002/aic.18595>.  
This review examines impinging jet mixers, detailing their fluid-dynamic mixing behavior, key performance factors, and design considerations. It also surveys their applications across chemical and pharmaceutical processes, highlighting advantages for rapid micromixing and reactive crystallization.
23. Woo XY, Tan RBH, Braatz RD: **Modeling and computational fluid dynamics–population balance equation–micromixing simulation of impinging jet crystallizers.** *Cryst Growth Des* 2009, **9**:156-164, <https://doi.org/10.1021/cg800095z>
24. Shin S, Devos C, Udepurkar AP, Inguva PK, Myerson AS, Braatz RD: **Mechanistic modeling of lipid nanoparticle (LNP) precipitation via population balance equations (PBEs).** *Chem Eng J* 2025, **523**:167786, <https://doi.org/10.1016/j.cej.2025.167786>
25. Raponi A, Fida D, Vicari F, Cipollina A, Marchisio D: **Computational fluid dynamics and population balance model enhances the smart manufacturing and performance optimization of an innovative precipitation reactor.** *Processes* 2025, **13**:1721, <https://doi.org/10.3390/pr13061721>
26. Garcia-Villalba M, Colonius T, Desjardins O, Lucas D, Mani A, Marchisio D, et al.: **Numerical methods for multiphase flows.** *Int J Multiphase Flow* 2025, **191**:105285, <https://doi.org/10.1016/j.ijmultiphaseflow.2025.105285>.  
This publication reviews the most recent advances in numerical methods for multiphase CFD. Part of the publication is specifically devoted to reactive solid-liquid flows, crystallization, and precipitation processes.
27. Marchioli C, Bourgoin M, Coletti F, Fox R, Magnaudet J, Reeks M, et al.: **Particle-laden flows.** *Int J Multiphase Flow* 2025, **191**:105291, <https://doi.org/10.1016/j.ijmultiphaseflow.2025.105291>.  
This article reviews the physics, modeling, and simulation of particle-laden flows, covering particle–fluid interactions across regimes. It highlights recent advances and challenges in predicting dispersion, collisions, and turbulence effects in complex multiphase systems.
28. Fox RO: **The particle–fluid–particle pressure tensor for ideal-fluid–particle flow.** *J Fluid Mech* 2025, **1010**:A8, <https://doi.org/10.1017/jfm.2025.333>
29. Fox RO: **Recent advances in well-posed Eulerian models for polydisperse multiphase flows.** *Int J Multiphase Flow* 2024, **172**:104715, <https://doi.org/10.1016/j.ijmultiphaseflow.2023.104715>
30. Fox RO: **A kinetic-based hyperbolic two-fluid model for binary hard-sphere mixtures.** *J Fluid Mech* 2019, **877**:282-329, <https://doi.org/10.1017/jfm.2019.608>
31. Raponi A, Romano S, Battaglia G, Buffo A, Vanni M, Cipollina A, et al.: **Computational modeling of magnesium hydroxide precipitation and kinetics parameters identification.** *Cryst Growth Des* 2023, **23**:4748.
32. Raponi A, Achermann R, Romano S, Trespi S, Mazzotti M, Cipollina A, et al.: **Population balance modelling of magnesium hydroxide precipitation: full validation on different reactor configurations.** *Chem Eng J* 2023, **477**:146540.
33. Hansson J, Lichtenegger T, Pirker S, Sasic S, Ström H: **Recurrence computational fluid dynamics for efficient predictions of long-term particle deposition on a cylinder.** *Phys Fluids* 2025, **37**:093320, <https://doi.org/10.1063/5.0283431>.  
Recurrence CFD is shown to predict particle deposition on a cylinder with accuracy comparable to full CFD but at a drastically lower computational cost. Front-side deposition is captured reliably across Reynolds numbers, while back-side prediction depends on database length, enabling major acceleration of deposition studies.
34. Lichtenegger T, Pirker S: **Recurrence CFD—a novel approach to simulate multiphase flows with strongly separated time scales.** *Chem Eng Sci* 2016, **153**:394.

35. Pedregosa F, Varoquaux G, Gramfort A, Michel V, Thirion B, Grisel O, et al.: **Scikit-learn: machine learning in Python.** *J Mach Learn Res* 2011, **12**:2825.
36. Borsos Á, Hámori C, Szilágyi E, Spaitz A, Farkas F, Százdi L, et al.: **Derisking crystallization process development and scale-up using a complementary, “Quick and Dirty” digital design.** *Org Process Res Dev* 2024, **28**:3813–3826, <https://doi.org/10.1021/acs.oprd.4c00199>.
- The study proposes combining DoE experiments with an application-focused crystallization model, using DoE data to calibrate and validate the model and then overlapping the two design spaces to obtain a de-risked, more reliable process window. Demonstrated on a fed-batch salting-out crystallization, the approach improves robustness, supports scale-up to manufacturing scale, and adds no risk since traditional DoE results remain available even if modeling falls short.
37. Orosz Á, Sandor L, Firoozirad K, Pusztai E, Nagy-Gyorgy P, Szilagyí B: **Streamlining crystallization process scale-up using statistical modeling of experiments and complementary CFD flow fields.** *Powder Technol* 2025, **458**:120934, <https://doi.org/10.1016/j.powtec.2025.120934>.
- The paper introduces a simple, data-driven method that links CFD simulations with experiments to support rapid, practical scale-up when stirring conditions are the main focus. Using small-scale crystallization experiments and CFD simulations, predictive CFD variables affecting product quality were identified with PLS-based feature selection. Five shear-related CFD variables enabled accurate prediction of particle size distributions at a larger scale, showing the method's effectiveness for flow-centric scale-up problems.
38. Xiouras C, Cameli F, Quilló GL, Kavousanakis ME, Vlachos DG, Stefanidis GD: **Applications of artificial intelligence and machine learning algorithms to crystallization.** *Chem Rev* 2022, **122**:13006–13042, <https://doi.org/10.1021/acs.chemrev.2c00141>.
- This review surveys how AI and machine learning are being applied across crystallization science, from nucleation prediction and polymorph screening to process monitoring and control. It highlights recent advances, challenges, and opportunities for data-driven methods to accelerate crystallization design, optimization, and scale-up.
39. Raponi A, Marchisio D: **Multivariate optimization and inverse design of multiphase reactive systems via deep learning and 3D CFD–PBM simulations.** *Chem Eng J* 2026, **531**:173908, <https://doi.org/10.1016/j.cej.2026.173908>
40. Raponi A, Marchisio D: **Deep learning for kinetics parameters identification: a novel approach for multi-variate optimization.** *Chem Eng J* 2024, **489**:151149, <https://doi.org/10.1016/j.cej.2024.151149>.
- In this publication, neural networks are employed to surrogate a computational flow model for crystallization. The neural network is then flipped out to generate the so-called mirror model to infer missing model parameters.
41. Raponi A, Marchisio D: **Multivariate optimization and inverse design of multiphase reactive systems via deep learning and 3D CFD–PBM simulations.** *Chem Eng J* 2026, **531**:173908, <https://doi.org/10.1016/j.cej.2026.173908>
42. Raponi A, Fida D, Vicari F, Cipollina A, Marchisio D: **Computational fluid dynamics and population balance model enhances the smart manufacturing and performance optimization of an innovative precipitation reactor.** *Processes* 2025, **13**:1721, <https://doi.org/10.3390/pr13061721>
43. Para ML, Alidoost M, Shiea M, Boccardo G, Buffo A, Barresi AA, et al.: **A modelling and experimental study on the co-precipitation of Ni<sub>0.8</sub>Mn<sub>0.1</sub>Co<sub>0.1</sub>(OH)<sub>2</sub> as precursor for battery cathodes.** *Chem Eng Sci* 2022, **254**:117634.
44. Tsuchioka K, Hayashi K, Misumi R: **Method for predicting the size of Ni<sub>1/3</sub>Mn<sub>1/3</sub>Co<sub>1/3</sub>(OH)<sub>2</sub> particles precipitated in a stirred-tank semi-batch crystallizer using CFD and particle agglomeration models.** *Heliyon* 2024, **10**:e28710, <https://doi.org/10.1016/j.heliyon.2024.e28710>
45. Xu D, Zhang H, Zhang L, Xiao H, Chen A, Xu W, et al.: **Reactive crystallization regulation for synthesizing NCM811 precursor by different impellers.** *J Alloy Compd* 2024, **1008**:176775, <https://doi.org/10.1016/j.jallcom.2024.176775>.
- In this publication, new impeller designs for a reactive crystallization process were tested using CFD. Simulations revealed that FPT-6 enhances nucleation while PFDT promotes crystal growth in precursor formation. Tailoring nucleation and growth with specific impeller combinations greatly improved precursor density, sphericity, and high-rate electrochemical performance. Dual-impeller setups produced dense, smooth particles and better cycle retention, offering a scalable strategy for optimizing cathode precursor synthesis.
46. Raponi A, Marchisio D: **Multivariate optimization and inverse design of multiphase reactive systems via deep learning and 3D CFD–PBM simulations.** *Chem Eng J* 2026, **531**:173908, <https://doi.org/10.1016/j.cej.2026.173908>
47. Raponi A, Fida D, Vicari F, Cipollina A, Marchisio D: **Computational fluid dynamics and population balance model enhances the smart manufacturing and performance optimization of an innovative precipitation reactor.** *Processes* 2025, **13**:1721, <https://doi.org/10.3390/pr13061721>
48. Lavino AD, Ferrari M, Barresi AA, Marchisio D: **Effect of different good solvents in flash nano-precipitation via multi-scale population balance modeling-CFD coupling approach.** *Chem Eng Sci* 2021, **245**:116833, <https://doi.org/10.1016/j.ces.2021.116833>
49. Schikarski T, Trzenschiok H, Avila M, Peukert W: **Impact of solvent properties on the precipitation of active pharmaceutical ingredients.** *Powder Technol* 2023, **415**:118032, <https://doi.org/10.1016/j.powtec.2022.118032>.
- A simulation framework is used to isolate how mixture-dependent viscosity, density, diffusion, and solubility influence antisolvent precipitation in different mixer designs. The model accurately predicts full particle size distributions of Ibuprofen nanoparticles across solvents and conditions, matching experiments closely.
50. Dong J, Wu Y, Liu X, Zhang C, Wang S, Wen J: **CFD-PBE Simulation of para-Xylene crystallization behavior and process amplification under different operating conditions.** *Ind Eng Chem Res* 2023, **62**:14657–14670, <https://doi.org/10.1021/acs.iecr.3c01272>
51. Kim SH, Hong MS, Braatz RD: **Investigation of particle flow effects in slug flow crystallization using the multiscale computational fluid dynamics simulation.** *Chem Eng Sci* 2024, **297**:120238, <https://doi.org/10.1016/j.ces.2024.120238>.
- A new CFD model (MVP) combining MP-PIC, VOF, and PBE is developed and validated, accurately predicting three-phase slug-flow crystallization and particle size changes. Case studies show it can capture slug-length effects, particle mixing, and hydrodynamics, offering a powerful tool for intensifying crystallization processes.
52. Achermann R, Antunes Morgado N, Corti AL, Mazzotti M: **Comparative assessment and possible applications of three models of Taylor slug flows.** *Comput Chem Eng* 2022, **161**:107773, <https://doi.org/10.1016/j.compchemeng.2022.107773>
53. Achermann R, Adams R, Prasser HM, Mazzotti M: **Characterization of a small-scale crystallizer using CFD simulations and X-ray CT measurements.** *Chem Eng Sci* 2022, **256**:117697, <https://doi.org/10.1016/j.ces.2022.117697>.
- The study combines CFD simulations with X-ray CT imaging to characterize fluid flow and crystal distribution in a small-scale crystallizer. This integrated approach provides detailed insight into crystallizer performance, improving understanding and design of crystallization processes.
54. Achermann R, Wiedmeyer V, Hosseinalipour MS, Güngör S, Mazzotti M: **Model-based design of pressure-driven product removal from stirred suspensions.** *Chem Eng Res Des* 2021, **174**:57–70, <https://doi.org/10.1016/j.cherd.2021.07.001>
55. Ganjare A, Ranade V: **Strategies for managing clogging and encrustation in compact continuous crystallizers: anti-solvent crystallization of paracetamol with fluidic oscillator and helical coil.** *Chem Eng Sci* 2025, **305**:121102, <https://doi.org/10.1016/j.ces.2024.121102>